Cofactor Triggers the Conformational Change in Thymidylate Synthase: Implications for an Ordered Binding Mechanism†

Alexander Kamb, Janet S. Finer-Moore, and Robert M Stroud*

Department of Biochemistry and Biophysics, University of California, San Francisco, California 94143

Received May 22, 1992; Revised Manuscript Received October 5, 1992

ABSTRACT: We have solved crystal structures of two complexes with *Escherichia coli* thymidylate synthase (TS) bound either to the cofactor analog N^{10}-propargyl-5,8-dideazafolate (CB3717) or to a tighter binding polygutamyl derivative of CB3717. These structures suggest that cofactor binding alone is sufficient to induce the conformational change in TS; dUMP binding is not required. Because polyglutamyl folates are the primary cofactor form in vivo, and because they can bind more tightly than dUMP to TS, these structures may represent a key intermediate along the TS reaction pathway. These structures further suggest that the dUMP binding site is accessible in the TS–cofactor analog binary complexes. Conformational flexibility of the binary complex may permit dUMP to enter the active site of TS while the cofactor is bound. Alternatively, dUMP may enter the active site from the opposite side that the cofactor appears to enter; that is, through a portal flanked by arginines that also coordinate the phosphate group in the active site. Entry of dUMP through this portal may allow dUMP to bind to a TS–cofactor binary complex in which the complex has completed its conformational transition to the catalytically competent structure.

Thymidylate synthase (TS),[1] a homodimer with two active sites per enzyme molecule, catalyzes formation of dTMP by transfer of a methylene group and a hydride from a CH_2-H_4folate cofactor to dUMP. The reaction has been studied extensively in vitro and consists of several discrete steps in which TS binds its ligands, changes conformation, associates covalently with dUMP, and facilitates donation of a methyl group to the 5-position of dUMP (Santi & Danenberg, 1984; Finer-Moore et al., 1990). The order of some of these events depends on the structure of the cofactor. For example, kinetic experiments reveal that if monoglutamyl folate is used, the binding reaction is ordered. TS first binds dUMP and then folate (Danenberg & Danenberg, 1978; Daron & Aull, 1978). In phosphate buffer (but not in Tris hydrochloride buffer) using polyglutamyl folate, however, TS binds its ligands in a random fashion (Ghose et al., 1990). The polyglutamyl cofactor binds to either the dUMP-bound enzyme or the free enzyme.

Ligand binding triggers a dramatic conformational change in TS whereby the protein embraces dUMP and cofactor and sequesters them from solvent (Montfort et al., 1990; Matthews et al., 1990) Whether the cofactor and substrate together or the cofactor alone triggers the protein conformational change is not certain. Crystal structures of TS bound to dUMP are nearly identical to structures of unbound TS, suggesting that interaction between TS and dUMP does not induce the conformational change (Stroud et al., in preparation). In contrast, crystal structures of TS bound in ternary complex with both dUMP and folate (or folate analogs) show significant differences in the conformation of the protein compared to the unbound or dUMP-bound structures (Montfort et al., 1990; Matthews et al., 1990; Kamb et al., 1992); for example, in the ternary complex the C-terminus of TS moves 5 Å toward the active site. These results demonstrate that the cofactor is necessary to induce the conformational change that leads to a presumptive catalytically competent complex. The position of dUMP relative to cofactor in the ternary complex is consistent with a mechanism where TS binds dUMP before binding cofactor and releases dTMP product last: the cofactor lies nearest to the mouth of the active site with dUMP located behind.

The observation that TS can bind cofactor in the absence of dUMP suggests that the crystal structure of a TS–cofactor binary complex may provide insight into, first, the interactions that provoke the conformational change presumably required for catalysis, and second, the mechanism by which TS binds its ligands in a random order. We have solved the crystal structures of TS bound to either a monoglutamyl folate analog (CB3717; Figure 1) or a polyglutamyl analog that contains four glutamate residues linked via amide bonds through their γ-carboxyl groups (CB3717polyGlu). These cofactor analogs are close structural mimics of the normal cofactor. The two binary structures provide a view of a potential precatalytic complex in the TS reaction and help define factors that alter the conformation of the protein.

MATERIALS AND METHODS

Reagents. Purified *Escherichia coli* TS was provided by Drs. F. and G. Maley and was stored at –80 °C as an ammonium sulfate precipitate (Belfort et al., 1983). CB3717-polyGlu and CB3717 were from H. Calvert and ICI.

Crystallization. Crystallization of TS–CB3717 or TS–CB3717polyGlu complexes was carried out as described (Montfort et al., 1990; Perry et al., 1990). TS was dialyzed against 20 mM potassium phosphate (pH 7.0 or 8.0), 0.1 mM ethylenediaminetetraacetic acid (EDTA), and 10 mM dithiothreitol (DTT). A protein–ligand solution was prepared with TS (4.5 mg/mL), 2 mM CB3717polyGlu or 3 mM CB3717, 20 mM potassium phosphate (pH 7.0 or 8.0), and 10 mM DTT and incubated overnight at 4 °C. Crystals were grown

† Supported by National Institutes of Health Grants CA-41323 to J.S.F.-M. and R.M.S. and GM24485 to R.M.S. Crystallographic refinement was carried out at the Pittsburgh Supercomputer Center under Grant DMB890040P.

* Author to whom correspondence should be addressed.

[1] Abbreviations: CH_2-H_4folate, methylenetetrahydrofolate; TS, thymidylate synthase; dUMP, deoxyuridylate; PABA, *p*-aminobenzoic acid; dTMP, thymidylate; CB3717, 10-propargyl-5,8-dideazafolate; CB3717polyGlu, polyglutamyl CB3717; EDTA, ethylenediaminetetraacetic acid; DTT, dithiothreitol.

0006-2960/92/0431-12876$03.00/0

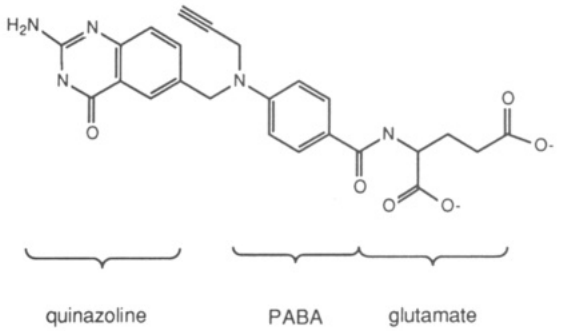

FIGURE 1: Folate analog CB3717. The polyglutamyl version of the analog has a total of four glutamate residues bound together through their γ-carboxyl groups.

by vapor diffusion in hanging drops after mixing a protein–ligand solution at different ratios ranging from 4:1 to 1:4 with well buffer consisting of 20 mM potassium phosphate (pH 7.0 or 8.0), 2.3 or 2.4 M ammonium sulfate, and 10 mM DTT to achieve a final volume of 5 μL/drop. Crystals grew over a 2-week interval. Prior to capillary mounting for X-ray crystallography, hexagonal rod crystals were transferred to depression wells containing 20 mM potassium phosphate (pH 8.0), 2.5 M ammonium sulfate, 0.1 mM EDTA, and 10 mM DTT. In both cases, TS–CB3717 and TS–CB3717polyGlu, the crystals were in the $P6_3$ space group with a dimer in the asymmetric unit and unit cell constants a = 127.3 Å and c = 68.2 Å.

X-ray Data Collection. For TS–CB3717 crystals, diffraction data were collected from a single crystal at room temperature using a Siemens IPC area detector on a three-circle goniometer. A CuKα X-ray beam from a 100-μm focus rotating-anode X-ray generator (Rigaku) with Franks mirrors was used. The oscillation width was 0.2° with 10 min of exposure time/deg of reciprocal space. Reflections were indexed and peak intensities were integrated using SCAN (Blum et al., 1987). Reflection intensities were scaled with one another by zonal scaling with SCALEI (Howard et al., 1985). The overall R_{sym} for all measured data to 2.2-Å resolution was 10.8%.

For TS–CB3717polyGlu crystals, data were collected using 1.08-Å synchrotron radiation at SSRL (Stanford, California) and Reflex 25 X-ray film (CEA, Sweden). Hexagonal rod crystals were aligned by eye with their long axis parallel to the ϕ axis of rotation. A single crystal was used for a complete set of data. Oscillations were 3° in ϕ per exposure. After six exposures, the crystal was translated 200 mm along its long axis and subjected to another six exposures in the X-ray beam. A total of 22 exposures were taken. Films were scanned and the peaks were digitized using a PDS microdensitometer (Perkin-Elmer). For each film an orientation matrix was obtained using the DENZO software package (Otwinowski, 1986) and the peak intensities were integrated. Partial reflections were excluded. Reflection intensities were merged and scaled together with the Rotavata/Agrovata software package from the CCP4 suite of programs (Daresbury, UK). The overall R_{sym} value for all film data was 9.6%.

Structure Solution, Refinement, and Model Building. The crystal structures were deduced from difference Fourier maps with phases calculated from the ternary complex of Montfort et al. (1990) but with the ligands removed from the model. Electron density maps were calculated using all data greater than 2σ. For the TS–CB3717 structure, we included data only to 3 Å because the average $I/\sigma(I)$ was less than 2.0 for the higher resolution data. The initial $(|F_o| - |F_c|)$, ϕ_{calc} and $(2|F_o| - |F_c|)$, ϕ_{calc} difference density maps contained considerable density in the active sites, but the quinazoline density was broken. Because the quinazoline conformation was ambiguous, the models were subjected to one round of refinement using X-PLOR (Brunger et al., 1987) energy minimization (150 cycles) followed by atomic B-factor refinement (40 cycles) before building the ligands into $(|F_o| - |F_c|)$, ϕ_{calc} difference Fourier maps. Further refinement cycles followed by calculation of $(2|F_o| - |F_c|)$, ϕ_{calc} electron density maps were used to reposition the ligands and to add water molecules. The original set of 213 waters was edited to remove waters clearly out of density in $(2|F_o| - |F_c|)$, ϕ_{calc} maps. Finally, the model was subjected to 1.35 ps of molecular dynamics. TS–CB3717polyGlu was refined using all nonzero data between 7- and 2.56-Å resolution. TS–CB3717 was refined using all collected data and the bulk solvent correction available in X-PLOR, except for the final refinement where no bulk solvent correction and only data between 7- and 3.0-Å resolution was used. Table II shows the refinement statistics for the two structures.

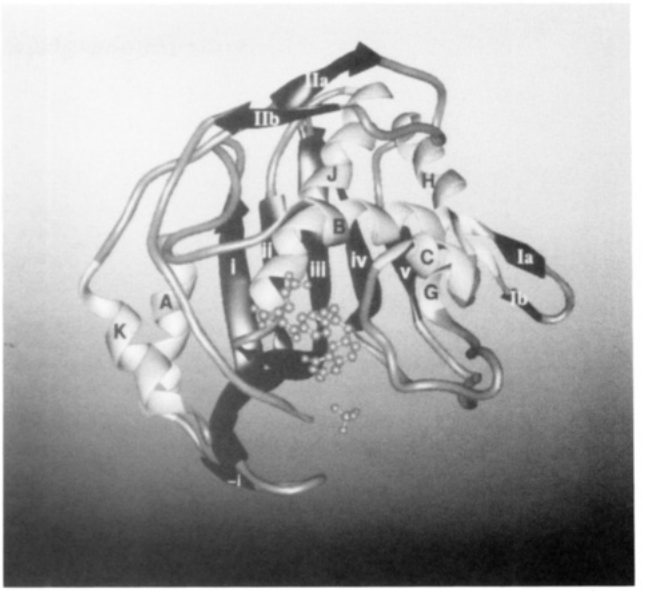

FIGURE 2: Ribbon drawing made with MidasPlus (Ferrin et al., 1988) of one monomer of TS–CB3717polyGlu, showing the nomenclature for secondary structure elements.

Structure Comparison. A suite of programs developed by E. Fauman and Robert Stroud (Perry et al., 1990; E. Fauman, unpublished work) were used to analyze the differences in atomic position among structures. The programs permit estimation of the statistical significance of these differences as a function of B-factor and resolution. Except where explicitly stated, the *E. coli* TS ternary complex used in these comparisons was from Montfort et al. (1990).

RESULTS

Conformation of TS in the Binary Complex. Our analysis of the TS–CB3717 and TS–CB3717polyGlu crystal structures shows that both cofactor analogs trigger the large conformational change seen in ternary complex formation (Figure 2). Unliganded *E. coli* TS and TS–dUMP crystallize in the same rhombic dodecahedral crystal form with a monomer in the asymmetric unit. Ternary complexes of *E. coli* TS with dUMP and either CB3717 (Montfort et al., 1990) or CB3717polyGlu (Kamb et al., 1992) crystallize in a different, hexagonal rod crystal form with a dimer in the asymmetric unit. Several crystallization drops of the TS–CB3717 or TS–CB3717polyGlu complexes contained crystal forms (rhombic

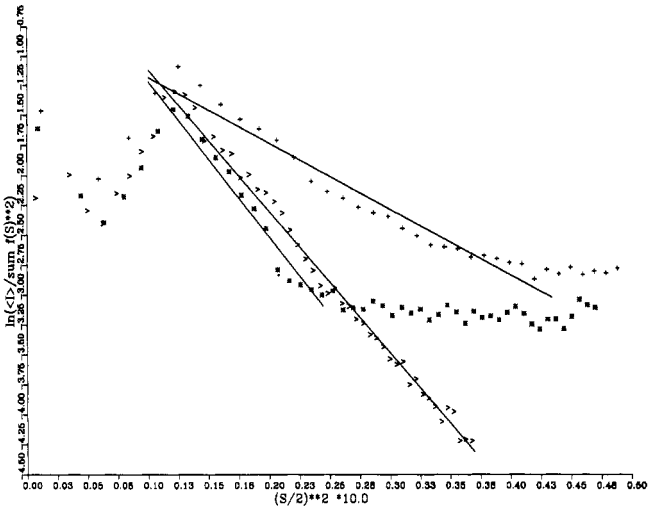

FIGURE 3: Wilson plots for TS–CB3717polyGlu (>), TS–CB3717 (*), and TS–dUMP–CB3717polyGlu (+).

dodecahedra) characteristic of unbound TS. However, in all cases these crystals remained small. The same drops also contained larger crystals with the morphology of ternary complex forms (hexagonal rods). Drops that were prepared using conditions most favorable to ternary complex crystal growth had hexagonal rods that were often hundreds of micrometers long and few if any rhombic dodecahedral crystals. This trend applied to crystallizations that involved either CB3717 or CB3717polyGlu. On the basis of the predominance of the hexagonal rod crystal forms, it seemed likely that the conformation of TS in these binary complex crystals would be similar to the configuration of the protein in ternary complex crystals.

The hexagonal rod crystal form of TS–CB3717 and TS–CB3717polyGlu had unit cell parameters within 0.5% of those for the crystals of TS–dUMP–CB3717 (Montfort et al., 1990) and TS–dUMP–CB3717polyGlu (Kamb et al., 1992). However, the TS–CB3717 and TS–CB3717polyGlu crystals were much more poorly ordered than the ternary complex crystals. The Wilson *B*-factors for TS–CB3717 and TS–CB3717polyGlu were 65 and 59 Å^2, respectively, compared to 27 Å^2 for the TS–dUMP–CB3717 and TS–dUMP–CE3717polyGlu data sets (Figure 3). The high symmetry *R*-factors (Table I) for the TS–CB3717 data for resolutions greater than 3.5 Å are a consequence of the fall-off in average intensity to background levels by 3-Å resolution. Data beyond 3-Å resolution were not included in refinement or electron density map calculations.

Data for TS–CB3717polyGlu were collected on film at the synchrotron, where lower backgrounds made it possible to collect reliable data out to 2.56-Å resolution. The symmetry *R*-factor for intensities between 2.63- and 2.56-Å resolution was 36.7% (Table I). Since there were, on average, three measurements of each independent reflection, this R_{sym} means that even the weak, highest resolution reflections had estimated errors in amplitudes of only $(37/2)/(3^{1/2}) = 10.6\%$. Most data had estimated errors of less than 5%. Assuming the phases for the crystal structure are all correct (figure of merit of 1.0), these uncertainties in amplitudes can be used to calculate an estimated noise level in difference maps of 0.06 electron/Å^3 (Henderson & Moffat, 1971). The estimated noise level of the TS–CB3717 structure is 0.04 electron/Å^3.

The TS–CB3717 and TS–CB3717polyGlu crystals were isomorphous with the TS–dUMP–CB3717 crystals, allowing us to solve the binary complex structures with the highly refined (R = 18% for all data to 2-Å resolution) structure of TS–dUMP–CB3717 (Montfort et al., 1990) (Table I). Starting phases for the binary complex structures were therefore excellent and *R*-factors of 16% and 18% were obtained without rebuilding the protein model, though the average *B*-factors were twice as high as in TS–dUMP–CB3717. In cases such as these, uncertainties in atomic position are small and are a function of atomic *B*-factor according to $\sigma_{xyz}(B) = 3/4rR(aB^2 + bB + c)$, where a, b, and c are empirically determined parameters for a given structure (Chambers & Stroud, 1979; Perry et al., 1990) (Figure 4). Thus, even for the 3-Å TS–CB3717 structure, the change in position of a typical atom (with an average *B*-factor of 28 Å^2) from its position in TS–dUMP–CB3717 (average B = 16 Å^2) can be estimated with an uncertainty of $\Delta r = \pm 0.24$ Å. The magnitude of the global conformational changes which characterize ternary complex formation in TS are much greater than this level of uncertainty: the rms deviation in α-carbon positions between unliganded TS and TS–dUMP–CB3717 is 0.99 Å and some residues move as much as 5 Å (Montfort et al., 1990). Since the protein conformation in TS–CB3717 and TS–CB3717-polyGlu is essentially the same, all our quantitative determinations of the altered conformation from unliganded TS used the higher resolution (2.56-Å) structure, TS–CB3717-polyGlu.

The difference between unbound and ternary structures reflects the combined effects of numerous shifts in atom position. There is a core of only 155 α-carbon atoms out of a total of 528 in the dimer whose distances from each other remain unchanged (±0.5 Å) through the conformational transition (Montfort et al., 1990). In contrast, the TS–CB3717polyGlu and ternary structures share a conserved core nearly twice as large: 324 α-carbons per dimer. Thus, the main chain of the TS–CB3717polyGlu binary complex resembles the ternary conformation much more closely than the unbound conformation. The rms difference between α-carbon positions of TS–CB3717polyGlu and TS–dUMP–CB3717 is 0.41 Å, a value similar to the rms deviation between α-carbons of the two, independently built monomers in TS–dUMP–CB3717, 0.37 Å. In contrast, the rms differences between α-carbon positions of TS–CB3717polyGlu and unliganded TS (after overlapping the structures) is 0.89 Å.

The transition from the unbound, open structure of *E. coli* TS to the closed, ternary structure involves a substantial closure of the enzyme around the ligands which can be expressed as additive vectorial movements of many structural domains comprising many atoms. The transition between the open and closed complex can be expressed as the summed effect of 21 segmental shifts of secondary structural elements (Montfort et al., 1990). To assess the extent of the conformational change which occurs on binding CB3717polyGlu (or CB3717) alone, we overlapped the common core α-carbon atoms of TS–CB3717polyGlu and unliganded *E. coli* TS and calculated the same 21 vectorial shifts. We also calculated the magnitude of vectorial segmental shifts between TS–CB3717polyGlu and TS–dUMP–CB3717 after overlapping their 324 constant core α-carbons. As shown in Table III, the shifts in secondary structure elements on binding CB3717polyGlu alone are very similar to the shifts which occur on binding both dUMP and CB3717. For 13 of the 21 segments, the shifts are more than twice as large as the segmental shifts between TS–

[2] By convention we use the *Lactobacillus casei* amino acid numbering scheme when referring to amino acid residues by number. The *E. coli* number follows in parentheses. For *E. coli* residues $1 \geq n \leq 89$, n(*L. casei*) = n(*E. coli*) + 2; for residues $n > 89$, n(*L. casei*) = n(*E. coli*) + 52.

Table I: Statistics for Crystallographic Data Collected on TS–CB3717polyGlu and TS–CB3717 Crystals[a]

resolution range (Å)	no. of collected reflections	% of possible reflections collected	no. of total observations	average $I/\sigma(I)$	R_{sym}[b] (%)	$R_{sym}(F)$[c] (%)	R_{crys}[d] (%)	R_{crys} (%) ternary[e]
			(A) TS–CB3717polyGlu					
∞–10.92	253	83.8	827	6.03	10.7	3		
10.92–7.82	460	89.8	1505	6.30	9.9	2.7		
7.82–6.41	568	94.0	1954	5.81	9.3	2.5	30.3	21.6
6.41–5.56	668	92.0	2387	5.87	8.8	2.3	18.4	17.4
5.56–4.98	744	86.8	2540	5.43	8.4	2.3	16.9	14.4
4.98–4.55	806	92.4	2687	6.38	8.1	2.2	12.6	12.3
4.55–4.22	871	83.2	2917	6.26	7.9	2.1	12.7	11.4
4.22–3.95	891	84.9	3035	7.18	7.2	2	13.9	12.1
3.95–3.72	897	77.1	3115	5.47	8.3	2.2	15.4	13
3.72–3.53	947	78.2	3345	5.69	8.5	2.3	16.3	13.5
3.53–3.37	970	87.5	3413	4.66	9.1	2.4	17.7	14.3
3.37–3.22	990	70.7	3466	5.11	9.6	2.6	19.6	15.6
3.22–3.10	1025	74.2	3519	5.11	11.2	3	21.0	17.7
3.10–2.99	1053	82.8	3580	4.83	13.1	3.5	22.3	17.6
2.99–2.89	1067	68.5	3529	3.93	16.3	4.5	24.1	19.1
2.89–2.79	1077	71.4	3506	3.06	21.4	5.9	25.1	19.4
2.79–2.71	1073	76.9	3416	2.48	25.6	7.2	27.3	20.6
2.71–2.63	1109	60.2	3410	1.95	30.6	8.7	31.1	20.5
2.63–2.56	1012	65.1	3071	1.70	36.7	10.6	36.1	21.8
∞–2.56	16481	77.2	55222	4.63	9.6	2.6	18.5	15.8
			(B) TS–CB3717					
∞–5.45	4994	92.8	6601	22.10	5.70	1.6	24.3	
5.45–4.33	3499	99.4	6027	18.90	6.00	1.8	11.1	
4.33–3.78	3783	86.9	3654	11.30	7.00	2.5	12.8	
3.78–3.43	3961	66.6	2589	5.00	21.40	7.9	16.9	
3.43–3.19	3615	63.8	2522	2.30	37.00	13.6	20.5	
3.19–3.00	2167	72.1	2894	1.70	43.70	15.8	22.1	
∞–3.00	22019	80.4	24287	11.60	7.70	2.5	16.8	

[a] In both cases the unit cell was identical to the ternary complex unit cell of Montfort et al. (1990): $P6_3$; $a = b = 127.3$ Å, $c = 68.2$ Å. [b] $R_{sym} = \{[\sum_{hkl}\sum_{i=1}^{N} w_i(I_{avg} - I_i)^2]/[\sum_{hkl}\sum_{i=1}^{N} w_i(I_i)^2]\}^{1/2}$ where $I_{avg} = 1/N\sum_{i=1}^{N} I_i$ and $w_i = 1/\sigma_i^2$. [c] $R_{sym}(F)$, the estimated average percent error in $|F_o|$, = $R_{sym}/[2(\text{redundancy})^{1/2}]$. [d] $R_{crys} = \sum||F_o| - |F_c||/|F_c|$. [e] R_{crys} for the TS–dUMP–CB3717 crystal structure, which was used for phasing the initial density maps, is given in (Section A). For TS–CB3717, although data were collected to 2.2-Å resolution, data higher than 3.0-Å resolution had an average $I/\sigma(I)$ of less than 2.0 and were not included in refinement and difference Fourier calculations.

Table II: Refinement Statistics for TS–CB3717polyGlu and TS–CB3717

parameters	TS–CB3717polyGlu	TS–CB3717
no. of atoms	4467	4519
no. of waters	87	104
no. of discretely disordered side chains	0	0
B-factor model	restrained, isotropic	restrained, isotropic
	Diffraction Agreement	
resolution (Å)	7.0–2.56	7.0–3.0
no. of reflections	17310	8900
σ cutoff	0	0
R_{crys} (%)	18.5	13.7
	Stereochemical Ideality	
bond lengths (Å)	0.016	0.018
bond angles (deg)	3.6	3.8
torsion angles (deg)	26.6	26.6
average *B* (Å^2)	36	28

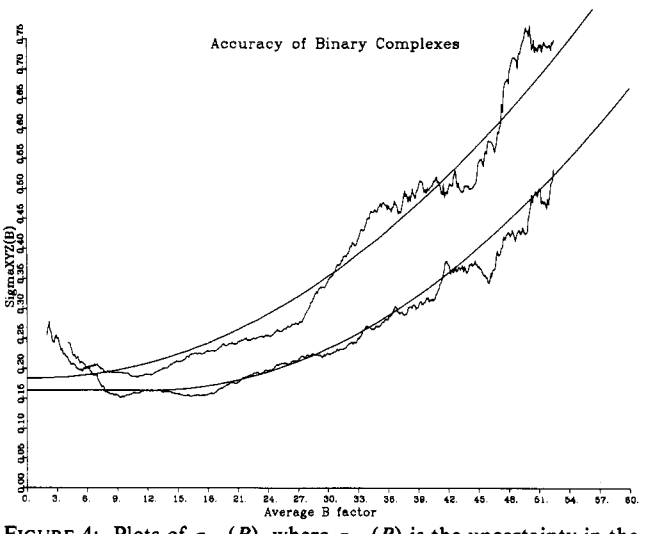

FIGURE 4: Plots of $\sigma_{xyz}(B)$, where $\sigma_{xyz}(B)$ is the uncertainty in the magnitude of positional differences between TS–dUMP–CB3717 and TS–CB3717 (top curve) or TS–CB3717polyGlu (bottom curve), as a function of the averaged *B*-factor of the compared atoms. The σ_{xyz} values are determined by binning the positional differences, Δr, according to averaged *B* and then fitting Gaussians to the Δr in each bin (Fauman et al., in preparation).

CB3717polyGlu and TS–dUMP–CB3717. Notably, segments 6 and 8 shift only about half as far into the active site in TS–CB3717polyGlu as in TS–dUMP–CB3717. These segments contain Trp-85 (83)[2] and Leu-195 (143), whose side chains pack against the quinazoline ring of CB3717 in both binary and ternary complexes, and Cys-198 (146), which covalently binds to dUMP in TS–dUMP–CB3717. The slight alteration in binding site of CB3717 in the TS–cofactor complexes relative to TS–dUMP–cofactor complexes (discussed in the next section) reduces closure of these segments around the active site.

The most dramatic conformational change on going from dUMP-bound or unbound TS to the ternary complex is the movement of the C-terminus into the active site where it forms hydrogen bonds with the N1 ring nitrogen of the CB3717 quinazoline via an ordered water, the guanidinium group of Arg-23 (21), and the ϵ-nitrogen of Trp-85 (83). In both the TS–CB3717 and the TS–CB3717polyGlu complexes, the C-terminus also moves into the active site and lies in a position where it may hydrogen bond with Arg-23 (21). However, in contrast to the ternary complex, neither the C-terminus nor

Table III: Segmental Shifts between Unliganded TS and TS–dUMP–CB3717, Unliganded TS and TS–CB3717polyGlu, and TS–CB3717polyGlu and TS–dUMP–CB3717[a]

segment	residue nos.	unliganded–ternary	unliganded–binary	binary–ternary
1	1–12	0.4	0.4	0.2
2	18–20	1.2	1.2	0.4
3	21–28	1.2	1.1	0.3
4	42–52	0.9	0.6	0.3
5	69–80	0.6	0.5	0.1
6	81–88	0.6	0.3	0.3
7	100–110	0.5	0.5	0.2
8	143–148	0.3	0.2	0.2
9	152–161	0.3	0.3	0.2
10	167–179	0.6	0.5	0.1
11	180–185	0.2	0.2	0.1
12	186–194	0.3	0.3	0.2
13	197–200	0.2	0.3	0.2
14	204–209	0.6	0.6	0.1
15	210–219	1.3	1.2	0.3
16	220–229	0.8	0.7	0.2
17	230–234	0.4	0.4	0.1
18	242–248	0.3	0.3	0.1
19	250–255	1.1	0.8	0.4
20	256–261	1.1	0.8	0.5
21	262–264	4.9	5.1	1.5

[a] Segmental shifts are given in angstroms and are the vector sums of shifts in α-carbon positions for the given residue range.

Arg-23 (21) is well-ordered (Figure 5). In monomer 1 of the TS–CB3717polyGlu structure, the average *B*-factor of atoms in the loop containing Arg-23 (21) and in C-terminal residues 314 (262)–316 (264) is over 2 times higher than the average *B*-factor of all monomer 1 atoms. In the ternary complex, *B*-factors for these atoms are approximately the same as the average *B*-factor for monomer 1. This same trend is also seen in monomer 2. In addition, the hydrogen bond between the terminal carboxylate and Trp-85 (83) is absent; the donor–acceptor atom centers are roughly 4 Å from each other. Instead, the terminal residue, Ile-316 (264), is rotated so that its aliphatic side chain packs against the quinazoline and the C-terminal carboxylate points into the solvent region. Thus, the C-terminus moves into the active site in forming the TS–cofactor analog binary complexes, but it is not as tightly confined as in the ternary complex and the C-terminal residue is rotated by nearly 180° around the Cα–Cβ bond.

The positions of amino acid side chains in the binary complexes are very similar to those in the ternary complex. Of all the atoms in the TS–CB3717polyGlu structure, including side-chain atoms, only 84 (2.0% of the total) differ in position from the ternary complex by more than $3\sigma_{xyz}$, where σ_{xyz} in an estimate of the positional error as a function of resolution, *R*-factor, and *B*-factor (Perry et al., 1990; Fauman et al., in preparation) (Figure 4). Excluding the C-terminus, the only large difference in side-chain motion common to both monomers is the His-53 (51) imidazole that lies on the surface in the B helix. This side chain is significantly less well ordered in the TS–CB3717polyGlu binary complex than in TS–dUMP–CB3717 (Montfort et al., 1990), TS–dUMP–CB3717polyGlu (Kamb et al., 1992), or the unbound structure (Perry et al., 1990). The side chains of Trp-82 (80) and Leu-195 (143), two residues that make hydrophobic contacts with the cofactor analog, are also moved. In both active sites of both complexes, TS–CB3717 and TS–CB3717polyGlu, the Leu-195 (143) side chain and the Trp-82 (80) side chain are rotated slightly to accommodate the quinazoline ring. In summary, the only significant differences in the structure of the protein in the binary complexes compared to the ternary complex are, first, the disorder of the C-terminus, Arg-23 (21) and His-53 (51); second, the rotation of the C-terminal Ile residue; and third, a slight reorganization of the hydrophobic cavity that surrounds the cofactor ring system.

Position of the Cofactor Analog in the Binary Complexes. Although much of the cofactor analog occupies the same position as in the ternary complex, the quinazoline ring differs slightly (Figure 6). In both active sites of the TS–CB3717polyGlu structure, the folyl glutamate, PABA ring, and propargyl group lie in strong electron density and are positioned as in the ternary structure. However, in the first active site, the quinazoline ring system is rotated approximately 40° such that it impinges upon the site that would be occupied by the deoxyribose group of dUMP (Figure 6). This rotation results in displacement of some atoms in the ring (e.g., Nα2) by 4.3 ± 0.5 Å from their position in the ternary complex. Other atoms in the ring near the axis of rotation, defined approximately by the C5–C6 bond, barely differ in position. For example, C5 differs by only 0.3 ± 0.5 Å from its position in the ternary complex. The binding in the two active sites is not symmetric in that the quinazoline ring is less ordered and is rotated further into the dUMP binding site in the second monomer than in the first. To best account for electron density of the quinazoline ring in the first active site of TS–CB3717, the quinazoline is modeled into two half-occupied partly overlapping positions: one position as described for the first active site in the TS–CB3717polyGlu complex and the other identical to the ternary conformation. In the second active site of TS–CB3717, the quinazoline is best modeled in a position intermediate between the quinazoline conformations of active sites 1 and 2 in the TS–CB3717polyGlu structure.

The quinazoline ring is less rigidly positioned in the TS–CB3717polyGlu binary complex than in the ternary complex. A diffuse lobe of density occupies the region of the quinazoline ring, suggesting that the ring is disordered (Figure 7). In the TS–CB3717 binary complex, electron density for the cofactor quinazoline ring is even more diffuse, indicating that the cofactor is less ordered than in the TS–CB3717polyGlu complex. For both TS–CB3717polyGu and TS–CB3717, *B*-factors of the quinazoline ring nitrogens (N1 and N3) are 2–3-fold higher than the average *B*-factor for all protein atoms. In contrast, N1 and N3 *B*-factors in the ternary complex are slightly lower than the average protein *B*-factor. These differences among atomic *B*-factors in the various structures indicate that the quinazoline ring is loosely bound in the TS–CB3717polyGlu complex compared to the ternary complex; in TS–CB3717, the quinazoline is even less constrained.

The polyglutamyl group is so poorly ordered in the TS–CB3717polyGlu binary complex that it was not visible in ($|F_o| - |F_c|$), ϕ_{calc} or ($2|F_o| - |F_c|$), ϕ_{calc} difference density maps. On the basis of biochemical cross-linking studies (Maley et al., 1982) and X-ray crystallography (Kamb et al., 1992), the polyglutamyl moiety is expected to lie near the B-helix. Comparison of B-helix residues in the two TS–cofactor analog binary complexes show one significant difference: the His-53 (51) imidazole is disordered in the TS–CB3717polyGlu structure. The disorder is attributable to the polyglutamate group because His-53 (51) lies in a clear region of electron density in the TS–CB3717 complex, ternary complex, and the unbound structure. Presumably the proximity of the polyglutamate disturbs the imidazole. In contrast, the less diffuse density of the cofactor analog in the TS–CB3717polyGlu structure compared to the TS–CB3717 structure probably results from the stabilizing effect of the polyglutamyl moiety on the complex. Even though electron density for the

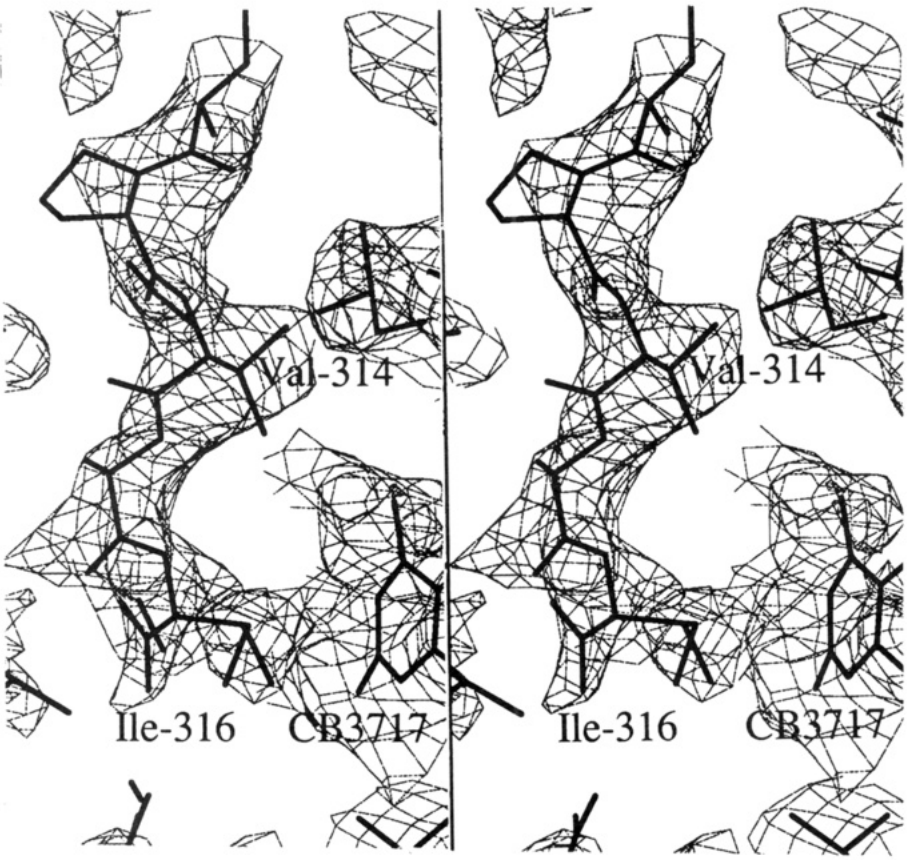

FIGURE 5: Divergent stereo drawing of electron density for the C-terminus of monomer 1 superimposed on the modeled structure for TS–CB3717polyGlu.

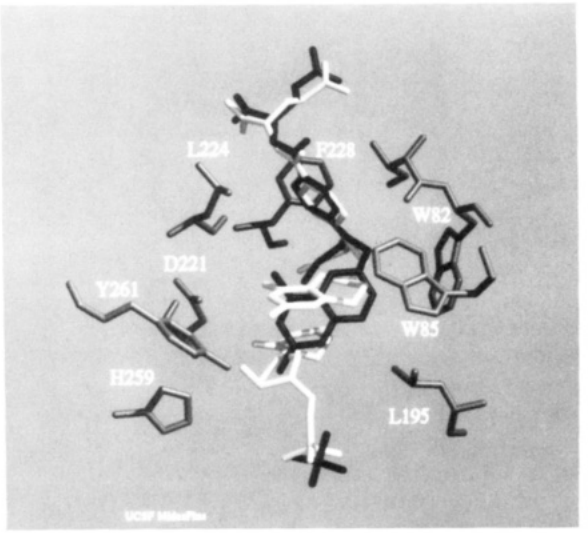

FIGURE 6: CB3717 conformation in the first active site of the TS–CB3717polyGlu binary complex. CB3717 and the phosphate of TS–CB3717polyGlu are shown in black. Relevant amino acid side chains that interact with the cofactor analog are shown in grey. The ligands of the TS–dUMP–CB3717 ternary complex (Montfort et al., 1990) are shown in white.

polyglutamyl group is not interpretable in difference Fourier maps, its presence is reflected in the increased order of CB3717 and the induced disorder of the His-53 (51) side chain.

Chemical Interactions between TS and the Cofactor Analog. The quinazoline ring of the cofactor in both TS–CB3717-polyGlu and TS–CB3717 does not form hydrogen bonds as in the ternary complex, but it makes hydrophobic contacts that are similar to the ternary complex interactions (Figure 6). As in the ternary complex, the quinazoline ring is surrounded by a pocket of hydrophobic residues [Trp-82 (80), Trp-85 (83), and Leu-195 (143)] in the binary complexes. Lacking, however, is the set of specific hydrogen bonds that coordinate the quinazoline ring in the ternary configuration: the N3 ring nitrogen interaction with Asp-221 (169), the N1 ring nitrogen interaction with the Ala-315 (263) carbonyl through a water molecule, and the hydrogen bonds between the quinazoline amino substituent and the Ala-315 (263) carbonyl and Asp-221 (169) through another water (Montfort et al., 1990). Instead, the amino substituent of the quinazoline in the binary complexes may hydrogen bond via an ordered water molecule to the hydroxyl group of Tyr-261 (209) and the Nϵ2 of His-259 (207), although disorder of the qinazoline prevents definitive assignment of these hydrogen bonds.

The most significant difference between the ternary and TS–cofactor analog binary complexes in terms of specific contacts with CB3717 involves dUMP. In the ternary structure, 9 of the 12 quinazoline ring atoms are within 3.8 Å of some part of dUMP (Montfort et al., 1990). Certain bonds compensate partly for the loss of dUMP interactions. For example, Tyr-261 (209) and His-259 (207), both of which form hydrogen bonds with the 3′-hydroxy group of dUMP in the ternary complex, may make new bonds with the cofactor.

Accessibility of the dUMP Binding Site. The dUMP binding site is surprisingly exposed in the closed conformation of TS. To estimate the accessibility of the dUMP binding site from outside the protein, we used a solvent accessibility algorithm (Connolly, 1983) and varied the probe sphere diameter. Coordinates for TS–dUMP–CB3717 (Montfort et al., 1990) with dUMP and water molecules removed were probed with spheres of diameter ranging from 2.4 to 3.8 Å. Spheres of diameter up to 3.6 Å were able to traverse the

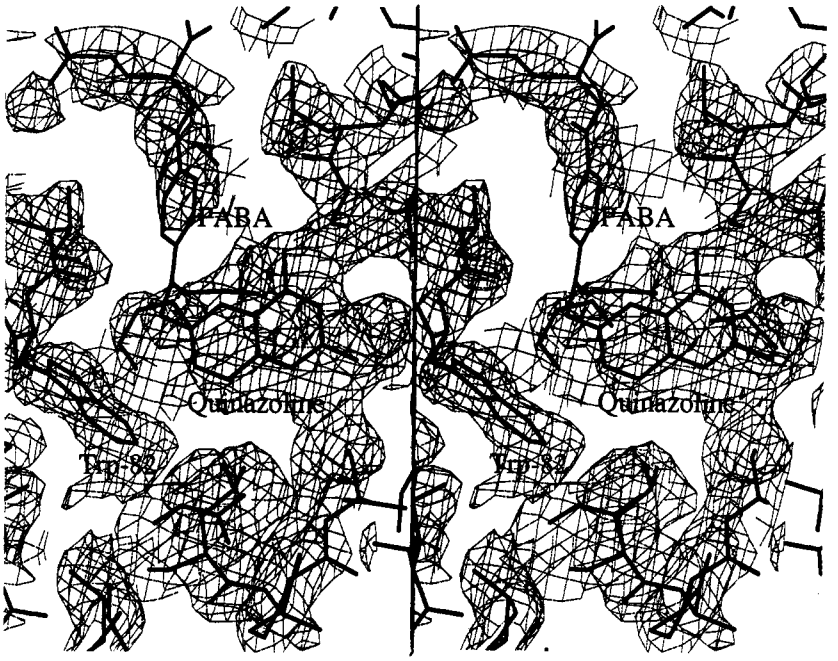

FIGURE 7: Divergent stereo drawing of electron density for the cofactor analog superimposed on the modeled structure in active site 1 for TS–CB3717polyGlu.

dUMP binding site and contact the quinazoline ring (data not shown). A similar analysis using coordinates for TS–CB3717polyGlu without water and inorganic phosphate showed that the quinazoline ring rotation slightly decreases accessibility of the dUMP side of the ring system. Spheres greater than 3.4 Å in diameter were not able to contact the quinazoline group. The route of entry of these spheres was not from the direction of the folyl glutamate; rather, it was from the opposite direction through a portal surrounded by residues Arg-23 (21) from monomer 1 and Arg-178(126) and Arg-179(127) from monomer 2. These arginines coordinate the phosphate group of dUMP in the ternary complex. The atoms flanking this portal form an entrance with the approximate shape of an equilateral triangle 6 Å on edge. Whereas CB3717 blocks access of the dUMP binding site from the folyl glutamate direction, the phosphate binding site offers a relatively open path.

DISCUSSION

Cofactor Binding Drives the TS Conformational Change. The TS–cofactor analog structures demonstrate that the TS conformational change can occur in the absence of dUMP. All the energy required to close the protein must be provided by cofactor binding. Several types of interaction may contribute to the forces that stabilize the closed form. In the TS–CB3717 and TS–CB3717polyGlu complexes, no specific contacts between the C-terminus and the quinazoline ring are apparent. However, even if such contacts exist, it is unlikely that they are necessary for the C-terminal conformational change: in an alternative form of the TS–dUMP–CB3717 complex in which some TS cysteines [e.g., Cys-220 (168) and Cys-244 (192)] are oxidized (Montfort et al., 1990), the C-terminus is drawn into the active site even though the quinazoline is rotated out of position to contact it. In the TS–CB3717 and TS–CB3717polyGlu complexes, the apparent disorder of residues 314 (262)–316 (264) suggests that the interaction between the C-terminus and the cofactor analog may not be strong. The C-terminal motion may involve a subtle perturbation in the electrostatic environment of the active site brought on by cofactor binding (Climie et al., 1992; Carreras et al., 1992). Such a change might shift the equilibrium so that the C-terminus is attracted more strongly into the active site.

In addition to the C-terminus, several other parts of the protein move to form the ternary complex. For example, the amino end of the long J helix moves by about 0.5 Å and the K helix on the protein surface moves about 1 Å upon binding ligands. Similar changes occur in the binary complexes. The energy required for these motions may derive from hydrophobic interactions such as those between Phe-228 (176) and the PABA ring as well as desolvation of the active site by the cofactor. The forces clearly do not involve hydrophobic or stacking interactions between the quinazoline ring and dUMP because dUMP is absent in the TS–cofactor analog complexes. Because of the intimate association between dUMP and cofactor in the ternary complex structure, it is surprising that dUMP does not play a larger role. Occupancy of the active site by CB3717 alone is sufficient to trigger most conformational motions characteristic of the open to closed transition in TS.

Effect of the Polyglutamyl Group on Cofactor Binding by TS. The intracellular pool of folates consists predominantly of polyglutamylated molecules with polyglutamyl groups of average length 4–7 depending on the cell type examined (McGuire & Coward, 1984). In contrast to the relatively low affinity of monoglutamyl folates for TS, polyglutamyl folates have affinities for TS that are in some cases over 400 times greater than that of the monoglutamyl form (Lu et al., 1984). Moreover, the affinities of both monoglutamyl and polyglutamyl cofactors depend on dUMP binding. For example, with monoglutamyl folate, the K_d drops from an undetectable level (>0.5 mM) in the absence of dUMP to 1.9 μM with dUMP (Galivan et al., 1976). With monoglutamyl cofactors, the reaction proceeds via an ordered binding mechanism with dUMP binding first, followed by cofactor binding (Danenberg & Danenberg, 1978). This results from the vastly greater binding affinity of dUMP for TS compared to the affinity of monoglutamyl folate for TS. However, with tetraglutamyl cofactors in phosphate buffer, the apparent binding order is random (Lu et al., 1984; Ghose et al., 1990). The polyglutamyl

group increases the affinity of tetraglutamyl folate for pig TS over 150-fold so that the cofactor binds in the absence of dUMP.

CB3717 is a close structural analog of the normal cofactor for TS, CH_2-H_4folate. CB3717 contains a benzene ring in place of the folate pyrazine ring and a propargyl group instead of a methylene (Figure 1). The conformation of CB3717 in the ternary complex is very similar to the conformation of folate in ternary complexes (Matthews et al., 1990; Stroud et al., in preparation). CB3717polyGlu is a variant that contains four glutamate residues instead of one. Both analogs are powerful inhibitors of TS. The tetraglutamyl group increases inhibitor binding to human TS 126-fold (Sikora et al., 1988). With *E. coli* TS, tetraglutamyl inhibitors are 67-fold more potent than monoglutamyl molecules (Friedkin et al., 1975).

Despite the significant binding energy contributed by the polyglutamyl moiety, the glutamate residues of CB3717polyGlu were not apparent in electron density maps of TS.CB3717-polyGlu. In contrast, the polyglutamyl moiety was visible in density maps of a TS–dUMP–CB3717polyGlu ternary complex (Kamb et al., 1992). This difference may reflect the mobility of the cofactor in the binary complex compared to the ternary complex. Comparison of average *B*-factors for the PABA ring atoms, for example, showed that in the binary complex *B*-factors are twice as high as the average *B*-factor of all protein atoms in the structure, whereas in the ternary complex, the average *B*-factor for PABA ring atoms is slightly less than the average *B*-factor for the protein. *B*-factors for atoms comprising the second and third glutamyl residues in the ternary complex are much higher: 3–4-fold higher than the average *B*-factor for the entire protein. Thus, in the binary complex the additional degree of mobility presumably precludes significant electron scattering contributions from the glutamates.

The structures of TS–CB3717 and TS–CB3717polyGlu are very similar to one another, indicating that the polyglutamyl moiety does not perturb the cofactor or the protein (with the exception of His-53) in the binary complex. The major difference between the complexes is the quality of electron density for the cofactor analog in the absence of polyglutamate. A single conformation of the quinazoline ring best accounts for the electron density in the first active site of the TS–CB3717polyGlu structure. In contrast, it is necessary to model the ring as two conformations in the first active site of the TS–CB3717 complex. Moreover, density for the cofactor is more diffuse and broken in the TS–CB3717 complex. Because the *R*-factor for the TS–CB3717 structure is low (13.7% for data between 7 and 3 Å) and the protein electron density is excellent, it is likely that the cofactor is more mobile than in the TS–CB3717polyGlu complex. Therefore, the polyglutamyl group acts mainly to constrain the motion of the cofactor but does not significantly affect its conformation or the conformation of the protein. This is consistent with a role for polyglutamate in considerably enhancing the binding affinity of cofactor for TS, while leaving V_{max}/K_m largely unaffected (Lu et al., 1984). The polyglutamyl group improves the binding of both the cofactor reactant and the cofactor product equally, increasing the association rate for the reactant while decreasing the dissociation rate of product. In vitro this change is manifested as an alteration of the order in which substrate and cofactor bind to TS: with polyglutamyl CH_2-H_4folate, cofactor can bind before dUMP and dissociate after dTMP (Lu et al., 1984; Ghose et al., 1990).

Relevance of the Binary Complex to the TS Reaction Mechanism. Most in vitro studies of the TS reaction mechanism have used monoglutamyl folate cofactors. In these cases, TS does not bind cofactor in the absence of dUMP. Thus the TS–cofactor binary complex does not contribute to the reaction process (Danenberg & Danenberg, 1978). However, when polyglutamyl cofactors are used, the increased affinity of cofactor for TS suggests that enzyme–cofactor binary complexes are a significant species in the reaction. Interestingly, both monoglutamyl CB3717 and polyglutamyl CB3717 crystallize in complex with TS. This demonstrates that a monoglutamyl cofactor analog that closely resembles the normal cofactor can bind TS without dUMP. CB3717 likely binds more tightly to TS free enzyme than CH_2-H_4-folate since it is a nanomolar inhibitor of the TS reaction (Pogolotti et al., 1986). However, under certain conditions in vitro, TS–CH_2-H_4folate complex may participate in the reaction and may be detectable by kinetic experiments. For instance, at high concentrations of cofactor, binding of cofactor to TS may decrease the association rate of dUMP by partly occluding the dUMP binding site.

Crystal structures provide a physical basis for considering the different outcomes that may follow TS–cofactor complex formation and suggest possible routes by which dUMP might bind to the binary complex. One possibility is that the open and closed conformations of the protein might be in euqilibrium with each other, allowing dUMP easy access during the intervals when the structure is open. Indeed, the disorder of residues 314 (262)–316 (264) suggests that the C-terminus is not bound tightly in the TS–cofactor analog crystal lattice. A second possibility is that dUMP may reach the active site without having to circumvent the cofactor even while the protein is in the closed conformation. The dUMP binding site is relatively exposed from the rear of the active site. The arginine residues that flank this entrance portal are highly conserved. Moreover, the atomic *B*-factors for one of these guanidinium groups [Arg-23 (21)] are unusually high. On the basis of their *B*-factors, some flanking atoms of the portal may experience a mean range of motion of nearly 1 Å. A phosphate group, which occupies the site in the ternary complex as a part of dUMP, is 5.2 Å wide along a tetrahedral edge between oxygen atoms. In the absence of a counterion, the guanidinium spacing would likely increase due to charge repulsion. Because a uracil ring is only 5.9 Å wide perpendicular to the N1–C4 axis, dUMP may pass to and from its binding site through the ring of arginines without difficulty. The disorder of the cofactor analog in the binary complexes suggests that the cofactor may be mobile enough to move out of the way of the incoming dUMP whether dUMP enters the active site from the front or from the rear.

CONCLUSION

Biochemical experiments have shown that the folate polyglutamyl group increases the binding affinity of cofactor for TS above the affinity of dUMP for TS. Thus polyglutamyl folate–TS complexes are relevant species in the reaction catalyzed by TS in vitro and perhaps also in vivo. It is possible to trap not only these polyglutamyl binary complexes in solution but also a complex between TS and monoglutamyl cofactor analog. This monoglutamyl binary complex may prove relevant under certain TS reaction conditions. The TS–cofactor analog binary structures suggest two scenarios for cases where TS binds cofactor before dUMP. First, cofactor may bind TS and stabilize marginally the closed conformation of the protein. This would allow dUMP to reach its binding site during the rapid conformational interconversions of the complex. Alternatively, dUMP may reach its binding site

through the phosphate binding site at the rear of the active site while the complex remains closed.

ACKNOWLEDGMENT

We are grateful to Louise Chang for assistance with synchrotron data collection and Partho Gosh for help with film data processing. We also thank Drs. F. and G. Maley for the gift of *E. coli* TS, Dr. H. Calvert, D. A. Slater, and Dr. L. Hughes for providing CB3717 and CF3717polyGlu, and Dr. D. Santi and C. Carreras for stimulating discussions and comments on the manuscript. Figures 2 and 6 were made by Julie Newdoll using the Midas Plus program written by Conrad Huang, Eric Pettersen, and Greg Couch at the UCSF Computer Graphics Laboratory.

REFERENCES

Belfort, M., Maley, G., & Maley, F. (1983) *Proc. Natl. Acad. Sci. U.S.A. 80*, 1858–1861.

Blum, M., Metcalf, P., Harrison, S. C., & Wiley, D. C. (1987) *J. Appl. Crystallogr. 20*, 235–242.

Brunger, A. T., Kuriyan, J., & Karplus, M. (1987) *Science 235*, 458–460.

Carreras, C. W., Climie, S. C., & Santi, D. V. (1992) *Biochemistry 31*, 6038–6044.

Chambers, J. L., & Stroud, R. M. (1979) *Acta Crystallogr., Sect. B 35*, 1861–1874.

Climie, S. C., Carreras, C. W., & Santi, D. V. (1992) *Biochemistry 31*, 6032–6038.

Connolly, M. L. (1983) *J. Appl. Crystallogr. 16*, 548–558.

Danenberg, P. V., & Danenberg, K. D. (1978) *Biochemistry 17*, 4018–4024.

Daron, H. H., & Aull, J. L. (1978) *J. Biol. Chem. 253*, 940–945.

Ferrin, T. E., Huang, C. C., Jarvis, L. E., & Langridge, R. (1988) *J. Mol. Graphics 6*, 2–12.

Finer-Moore, J. S., Montfort, W. M., & Stroud, R. M. (1990) *Biochemistry 29*, 6977–6986.

Friedkin, M., Plante, L., Crawford, E. J., & Crumm, M. (1975) *J. Biol. Chem. 250*, 5614–5621.

Galivan, J. H., Maley, G. F., & Maley, F. (1976) *Biochemistry 15*, 356–362.

Ghose, C., Oleinick, R., Matthews, R. G., & Dunlap, R. B. (1990) in *Chemistry and Biology of Pteridines 1989* (Curtius, H.-Ch., Ghisla, S., & Blau, N., Eds.) pp 860–865, Walter de Gruyter and Company, Berlin.

Henderson, R., & Moffat, J. K. (1971) *Acta Crystallogr., Sect. B 27*, 1414–1420.

Howard, A. J., Neilson, C., & Xuong, Ng. H. (1985) *Methods Enzymol. 114*, 452–472.

Kamb, A., Finer-Moore, J., Calvert, A. H., & Stroud, R. M. (1992) *Biochemistry 31*, 9883–9890.

Lu, Y.-Z., Aiello, P., & Matthews, R. (1984) *Biochemistry 23*, 6870–6876.

Maley, G. F., Maley, F., & Baugh, C. M. (1982) *Arch. Biochem. Biophys. 216*, 551–558.

Matthews, D. A., Villafranca, J. E., Janson, C. A., Smith, W. W., Welsh, K., & Freer, S. (1990) *J. Mol. Biol. 214*, 937–948.

McGuire, J. J. & Coward, J. K. (1984) in *Folates and Pterins: Volume 1—Chemistry and Biochemistry of Folates* (Blakley, R. L., & Benkovic, S. J., Eds.) pp 135–190, John Wiley and Sons, Inc., New York.

Montfort, W. R., Perry, K. M., Fauman, E. B., Finer-Moore, J. S., Maley, G. F., Hardy, L., Maley, F., & Stroud, R. M. (1990) *Biochemistry 29*, 6964–6977.

Otwinowski, Z. (1986) DENZO, University of Chicago.

Perry, K. M., Fauman, E. B., Finer-Moore, J. S., Montfort, W. R., Maley, G. F., Maley, F., & Stroud, R. M. (1990) *Proteins: Struct., Funct., Genet. 8*, 315–333.

Pogolotti, A. L., Jr., Danenberg, P. V., & Santi, D. V. (1986) *J. Med. Chem. 29*, 478–482.

Santi, D. V., & Danenberg, P. V. (1984) in *Folates and Pterins: Volume 1—Chemistry and Biochemistry of Folates* (Blakley, R. L., & Benkovic, S. J., Eds.) pp 345–398, John Wiley and Sons, Inc., New York.

Sikora, E., Jackman, A. L., Newell, D. R., & Calvert, A. H. (1988) *Biochem. Pharmacol. 37*, 4047–4054.